

# Geometric density of states of electronic structures for local responses: Phase information from the amplitudes of STM measurement

Shu-Hui Zhang<sup>1,\*</sup>, Jin Yang<sup>2</sup>, Ding-Fu Shao<sup>3</sup>, Jia-Ji Zhu<sup>4</sup>, Wen Yang<sup>2,†</sup> and Kai Chang<sup>5‡</sup>

<sup>1</sup>College of Mathematics and Physics, Beijing University of Chemical Technology, Beijing, 100029, China

<sup>2</sup>Beijing Computational Science Research Center, Beijing 100193, China

<sup>3</sup>Key Laboratory of Materials Physics, Institute of Solid State Physics, HFIPS, Chinese Academy of Sciences, Hefei 230031, China

<sup>4</sup>School of Science, Chongqing University of Posts and Telecommunications, Chongqing 400061, China and

<sup>5</sup>SKLSM, Institute of Semiconductors, Chinese Academy of Sciences, Beijing 100083, China

Electronic band structures underlie the physical properties of crystalline materials, their geometrical exploration renovates the conventional cognition and brings about novel applications. Inspired by geometry phases, we introduce a geometric amplitude named as the geometric density of states (GDOS) dictated by the differential curvature of the constant-energy contour. The GDOS determines the amplitude of the real-space Green's function making it attain the ultimate expression with transparent physics. The local responses of crystalline materials are usually formulated by the real-space Green's function, so the relevant physics should be refreshed by GDOS. As an example of local responses, we suggest using scanning tunneling microscopy (STM) to characterize the surface states of three-dimensional topological insulator under an in-plane magnetic field. The GDOS favors the straightforward simulation of STM measurement without resorting to Fourier transform of the real-space measurement, and also excavates the unexplored potential of STM measurement to extract the phase information of wavefunction through its amplitude, i.e., the spin and curvature textures. Therefore, the proposed GDOS deepens the understanding of electronic band structures and is indispensable in local responses, and it should be universal for any periodic systems.

*Introduction.*—As a successful application of quantum mechanics, the electronic band theory was developed to describe the motion of electrons or quasiparticles in crystalline materials with periodic structures in real space. The conventional electronic band theory describes the relation of energies and momenta of quasiparticles, i.e., the electronic band structure underlying the mechanical, thermal, optical and electrical properties of crystalline materials<sup>1</sup>. The profound insights into the band structure flourish into the modern band theory with geometrical phase<sup>2,3</sup> as an outstanding example. Geometrical phase embodies the geometrical information of band structure and is responsible for Berry physics and various novel phenomena<sup>4</sup>. At present, geometrical phase has become an essential ingredient of band structure, this inspires us to discover the analogous concept.

The macroscopic and global measurement, e.g., various Hall transport experiments, is usually used to reveal Berry physics since Berry curvature intrinsically provides an overall perspective of the electronic band structure<sup>5</sup>. Conversely, the local measurement is expected to reflect the local information of crystalline materials, which is strongly required in the field of low-dimensional physics<sup>6,7</sup>. Recently, two experiments use scanning tunneling microscopy (STM) to measure the Friedel oscillation (FO) induced by intentional introduced single impurity, then count the wavefront dislocations with the specific number corresponding to the Berry phase of monolayer and bilayer graphene<sup>8,9</sup>. Thus, these two experiments also demonstrate the possibility to extract the global Berry phase<sup>10</sup>. Hence, comparing to the global measurement, the local measurement provides information with higher complexity helpful to build the physical understanding of the novel materials. Furthermore, there are emergent non-magnetic, magnetic, topological two-dimensional (2D) materials and exotic surface states of three-dimensional topological

insulators and semimetals, their novel physics and potential applications<sup>11–17</sup> promote the ever-increasing demand of local information.

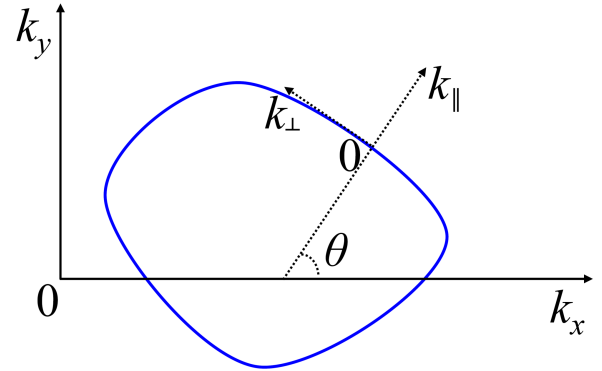


FIG. 1. Two coordinate systems and their relation. Choosing an energy  $\varepsilon$ , a general constant-energy contour is given through the energy dispersion, i.e.,  $E(\mathbf{k}) = \varepsilon$ , for the two-dimensional quasiparticles with the momentum  $\mathbf{k} = (k_x, k_y)$  in the coordinate system  $k_x - k_y$ . The gradient of constant-energy contour or the group velocity  $\mathbf{v} = \nabla E(\mathbf{k})$  helps define the unit vectors  $\mathbf{n}_{\parallel} = \mathbf{v}/|\mathbf{v}|$  and  $\mathbf{n}_{\perp} = \mathbf{z} \times \mathbf{v}/|\mathbf{v}|$  with  $\mathbf{z}$  pointing outside of the plane. And  $\theta$  is the azimuthal angle of  $\mathbf{v}$ . Thus, a local coordinate system  $k_{\parallel} - k_{\perp}$  is constructed, in which  $k_{\parallel} = \mathbf{k} \cdot \mathbf{n}_{\parallel}$  and  $k_{\perp} = \mathbf{k} \cdot \mathbf{n}_{\perp}$ .

In this study, we provide a local perspective of the electronic band structure by introducing microscopic description on the density of states (DOS). The conventional DOS provides a shortcut to catch the useful information from the electronic structure, which may be the most important concept for

understanding physical properties of crystalline materials and is formulated in undergraduate textbooks<sup>18</sup>. The microscopic DOS is dictated by the differential curvature of the constant-energy contour (CEC) of band structure, then is called geometric DOS (GDOS), which represents one kind of geometrical amplitude in contrast to geometrical phase<sup>4</sup>. The GDOS governs the amplitude of the real-space Green's function (GF) and makes it attain the ultimate expression with transparent physics. Since the local responses of crystalline materials are formulated by the real-space GF, the GDOS concept must refresh the understanding of previous local physical properties<sup>6,7,19–27</sup>. As an application for simulating STM experiment, we explore the possible modification of the electronic band structure of the surface states of three-dimensional topological insulator by an in-plane magnetic field<sup>28–30</sup>, which is blind for angle-resolved photoemission spectroscopy<sup>6</sup>. The GDOS, through the amplitude of real-space GF, provides a novel protocol to understand the STM measurement. More importantly, the GDOS dictates the STM detection of phase information, namely spin and curvature textures, through the amplitudes. Therefore, the proposed GDOS is a pivotal concept for the electronic structure and useful for the local responses, and should also be universal in any periodic systems.

*Definition of geometric density of states.*—Fig. 1 shows a general CEC  $E(\mathbf{k}) = \varepsilon$  for the 2D quasiparticles with the momentum  $\mathbf{k} = (k_x, k_y)$  in the coordinate system  $x - y$ . The gradient of the CEC is the group velocity  $\mathbf{v} = \nabla_{\mathbf{k}}E(\mathbf{k})$ . As shown by Fig. 1, a local coordinate system  $k_{\parallel} - k_{\perp}$  is constructed through  $k_{\parallel} = \mathbf{k} \cdot \mathbf{n}_{\parallel}$  and  $k_{\perp} = \mathbf{k} \cdot \mathbf{n}_{\perp}$  by using  $\mathbf{n}_{\parallel} = \mathbf{v}/|\mathbf{v}|$  and  $\mathbf{n}_{\perp} = \mathbf{z} \times \mathbf{v}/|\mathbf{v}|$ . The conventional DOS is defined as  $\rho_0(\varepsilon) \equiv \lim \delta N / \delta \varepsilon^1$ , in which  $\delta N$  represents the number of states in the energy range  $\delta \varepsilon$ . In analogy to  $\rho_0(\varepsilon)$ , we introduce the microscopic DOS  $\rho(\varepsilon, \theta) \equiv \lim \delta N / (\delta \varepsilon \delta \theta)$  with  $\theta$  the azimuthal angle of the group velocity in the coordinate system  $x - y$ . From Fig. 1, we arrive at

$$\rho(\varepsilon, \theta) = \frac{1}{4\pi^2} \frac{\delta k_{\parallel} \delta s}{\delta \varepsilon \delta \theta} = \frac{1}{4\pi^2 v \kappa}, \quad (1)$$

due to the group velocity  $v = \lim \delta \varepsilon / \delta k_{\parallel}$  and the curvature of the CEC:

$$\kappa = \lim \delta \theta / \delta s, \quad (2)$$

with  $\delta s$  the curve length of the CEC. Since  $\rho(\varepsilon, \theta)$  is determined by the differential curvature  $\kappa$ , so it attains the name GDOS. There are two implications of Eq. (1). On one hand, it gives the simple calculation of the GDOS since  $\kappa$  is a well-known mathematical quantity<sup>31,32</sup>. On the other hand, it allows the measurement of  $\kappa$  in experiment as shown below, which is inherently interesting.

*Real-space Green's function.*—The key of local responses is the real-space GF<sup>33</sup>. To consider a 2D system with the Hamiltonian in the diagonal basis:

$$\mathcal{H}(\mathbf{k}) = \sum_{\lambda} E_{\lambda}(\mathbf{k}) |u_{\lambda}(\mathbf{k})\rangle \langle u_{\lambda}(\mathbf{k})|. \quad (3)$$

Here,  $\lambda$  denotes the band index,  $\mathbf{k} = (k_x, k_y)$  is the momentum in the coordinate system  $x - y$ ,  $E_{\lambda}(\mathbf{k})$  and  $|u_{\lambda}(\mathbf{k})\rangle$  are the

eigenvalues and eigenstates, respectively. The corresponding real-space GF is  $\mathcal{G}(\varepsilon, \mathbf{r}) = \sum_{\lambda} \mathbf{g}_{\lambda}(\varepsilon, \mathbf{r})$ , which is the sum of contributions from different energy bands:

$$\mathbf{g}_{\lambda}(\varepsilon, \mathbf{r}) = \iint d\mathbf{k} \frac{e^{i\mathbf{k}\cdot\mathbf{r}}}{4\pi^2} \frac{|u_{\lambda}(\mathbf{k})\rangle \langle u_{\lambda}(\mathbf{k})|}{(\varepsilon + i0^+) - E_{\lambda}(\mathbf{k})}. \quad (4)$$

To decompose  $\mathbf{k} \equiv (k_{\parallel}, k_{\perp})$  into one parallel component  $k_{\parallel}$  and one perpendicular component  $k_{\perp}$  with respect to  $\mathbf{r}$  (cf. Fig. 1), thus

$$\mathbf{g}_{\lambda}(\varepsilon, \mathbf{r}) = \int \frac{dk_{\perp}}{2\pi} \left( \int \frac{dk_{\parallel}}{2\pi} e^{ik_{\parallel}r} \frac{|u_{\lambda}(\mathbf{k})\rangle \langle u_{\lambda}(\mathbf{k})|}{(\varepsilon + i0^+) - E_{\lambda}(k_{\parallel}, k_{\perp})} \right). \quad (5)$$

Usually, the band index  $\lambda$  can be omitted by assuming that there is only one on-shell solution  $k_{\parallel,+}(k_{\perp})$  for  $E_{\lambda}(k_{\parallel}, k_{\perp}) = \varepsilon$  to ensure the group velocity  $v_{\parallel}(k_{\perp}) \equiv \partial_{k_{\parallel}}E(\mathbf{k})|_{k_{\parallel}=k_{\parallel,+}(k_{\perp})}$  along  $\mathbf{r}$  with assuming its component  $x > 0$ , i.e.,  $v_{\parallel}(k_{\perp})$  is positive or equivalently  $\text{Im} k_{\parallel,+} > 0$ . To perform the Taylor expansion about  $k_{\parallel}$  for  $E(\mathbf{k})$  near  $k_{\parallel,+}(k_{\perp})$ , i.e.,  $E(k_{\parallel}, k_{\perp}) \approx \varepsilon + v_{\parallel}(k_{\perp}) [k_{\parallel} - k_{\parallel,+}(k_{\perp})]$ , which helps finish the contour integral of  $\mathbf{g}(\varepsilon, \mathbf{r})$  over  $k_{\parallel}$  in the upper half complex plane:

$$\mathbf{g}(\varepsilon, \mathbf{r}) \approx \int \frac{dk_{\perp}}{2\pi} \frac{e^{ik_{\parallel,+}(k_{\perp})r}}{iv_{\parallel}} |u(k_{\parallel,+}, k_{\perp})\rangle \langle u(k_{\parallel,+}, k_{\perp})|. \quad (6)$$

Therefore, Eq. (6) implies that all right-going on-shell eigenstates (either traveling or evanescent) contribute to GF. In the stationary phase approximation<sup>34–36</sup> for large  $r$ , the contribution to Eq. (6) should be dominated by  $k_{\perp}$  near the saddle point  $k_{\perp,c}$  determined by solution of  $\partial_{k_{\perp}}k_{\parallel}(k_{\perp}) = 0$ . So the classical momenta can be defined, i.e.,  $\mathbf{k}_c \equiv (k_{\parallel,c}, k_{\perp,c})$  with  $k_{\parallel,c} \equiv k_{\parallel,+}(k_{\perp,c})$ . Furthermore, for the CEC,  $\kappa \equiv \partial_{k_{\perp}}^2 k_{\parallel,+}|_{k_{\perp,c}}$  gives the equivalent definition of Eq. (2) for the differential curvature<sup>31,32</sup>. To expand  $k_{\parallel,+}(k_{\perp})$  around  $k_{\perp,c}$  up to quadratic order  $k_{\parallel,+}(k_{\perp}) \approx k_{\parallel,c} + \kappa/2(k_{\perp} - k_{\perp,c})^2$ , this leads to

$$\mathbf{g}(\varepsilon, \mathbf{r}) \approx \frac{e^{ik_{\parallel,c}r}}{iv_c} \frac{e^{-i\pi/4}}{\sqrt{2\pi r}} |u(\mathbf{k}_c)\rangle \langle u(\mathbf{k}_c)|, \quad (7)$$

with  $v_c = v_{\parallel}(k_{\perp,c})$ . Here, we have used the Gaussian formula  $\int_{-\infty}^{\infty} e^{-\alpha x^2} dx = \sqrt{\pi/\alpha}$  with  $\alpha \in \mathbb{C}$  and  $\arg(\alpha) \in [-\pi/2, \pi/2]$ . Using Eq. (1), the above equation can be rewritten as

$$\mathbf{g}(\varepsilon, \mathbf{r}) \approx -ie^{ik_{\parallel,c}r - i\pi/4} \sqrt{\frac{2\pi\rho}{v_c r}} |u(\mathbf{k}_c)\rangle \langle u(\mathbf{k}_c)|, \quad (8)$$

which presents the ultimate transparent expression with clear physics for  $\mathbf{g}(\varepsilon, \mathbf{r})$ . Once the electronic structure is given, it is convenient to construct  $\mathbf{g}(\varepsilon, \mathbf{r})$ , including two processes; I) finding the stationary points  $\mathbf{k}_c = (k_{x,c}, k_{y,c})$  on the CEC  $E_{\lambda}(\mathbf{k}) = \varepsilon$  satisfying  $\mathbf{v}_c \parallel \mathbf{r}$  with  $\mathbf{v}_c$  the classic velocity, this provides simultaneously  $k_{\parallel,c}r = \mathbf{k}_c \cdot \mathbf{r}$  and  $v_c = |\mathbf{v}_c|$ . II) calculating  $\rho(\varepsilon, \theta)$  through Eq. (1). Eqs. (1) and (8) are our main results, later we use an example to show their specific applications.

*Characterizing the topological surface states at nonzero magnetic field.*—The surface states of topological material (TISS) are the intuitive reflection of the bulk-boundary

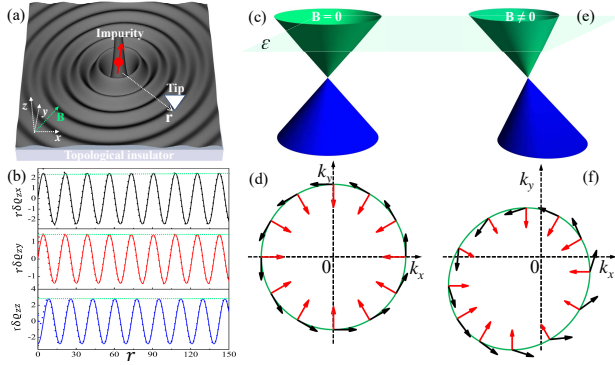


FIG. 2. A protocol to characterize topological surface states under an in-plane magnetic field. (a) For the surface states (black) on the three-dimensional topological insulator (light blue), a single magnetic impurity (red dot) at  $\mathbf{r} = \mathbf{0}$  is introduced intentionally. The impurity-induced Friedel oscillations (black oscillation waves), namely the change of the local density of states (LDOS) can be measured by spin-polarized scanning tunneling microscopy with the tip at  $\mathbf{r} \neq \mathbf{0}$  (white triangle), even under an in-plane magnetic field  $\mathbf{B}$ . The inset shows the coordinate system with  $\mathbf{B}$  lying in the  $x$ - $y$  plane. (b) Along an arbitrary direction, the change of LDOS  $r\delta\varrho_{zx}$  (black lines),  $r\delta\varrho_{zy}$  (red lines), and  $r\delta\varrho_{zz}$  (blue lines) are shown, which do not decay by accounting for the intrinsic  $1/r$  decay. In each panel, solid line and dotted line are, respectively, calculated by the  $T$ -matrix approach with and without Born approximation, they agree very well when  $r$  is longer than one oscillation wavelength. The green lines in all panels help extract the amplitudes  $r\delta\varrho_{a,zx}$ ,  $r\delta\varrho_{a,zy}$  and  $r\delta\varrho_{a,zz}$ , which determine the spin and curvature textures as shown in (d) and (f). In (b),  $v_F \equiv 1$ ,  $\theta_r = \pi/6$ ,  $\varepsilon = 0.15$ ,  $\mathcal{V} = 3$ , and  $t_x = t_y = 0.3$ . The in-plane  $\mathbf{B}$  modifies the electronic structure of topological surface states. The modification are clearly by showing the electronic structures at  $\mathbf{B} = \mathbf{0}$  (c) and  $\mathbf{B} \neq \mathbf{0}$  (e). Choosing the same Fermi levels  $\varepsilon$  (light green) in the (c) and (e), the constant-energy contour (CEC) is changed from the circle (d) into ellipse (f). The CECs are fringed by the spin texture (black) and the curvature texture (red), which can both be extracted through the STM measurement (see the text).

correspondence<sup>37</sup>, so it is a basic requirement to characterize the electronic properties of TISS under various fields. An in-plane magnetic field may lead to the drastic modification of the electronic structure of TISS, which brings about the novel effects such as the planar Hall effect<sup>28,29</sup> and the super-resonant transport<sup>30</sup>. It is promising to corroborate the modified TISS by an in-plane magnetic field, and there are two primary methods to characterize the electronic structure, i.e., angle-resolved photoemission spectroscopy (ARPES) and STM. But the conventional ARPES is incompatible with magnetic field<sup>23</sup>, so STM measurements become obligatory and there are a lot of STM experiments to visualize the surface states of topological materials<sup>6,23,38-47</sup>, but without considering the in-plane magnetic field. Here, we present a protocol to measure the FO induced by the imperfection on the surface of topological materials for characterizing the modified TISS [cf. Fig. 2(a)], and perform the theoretical analysis based on the ultimate expression of the real-space GF. The modified TISS by an in-plane magnetic field is described by the

Hamiltonian<sup>28,30,32</sup>:

$$\mathcal{H}(\mathbf{k}) = v_F(k_x\sigma_y - k_y\sigma_x) + \mathbf{t} \cdot \mathbf{k}. \quad (9)$$

Here,  $\sigma_{x,y}$  are Pauli matrices for the spin degrees of freedom,  $v_F$  is the velocity parameter and  $\mathbf{t} = (t_x, t_y)$  is the tilt vector induced by the applied in-plane magnetic field  $\mathbf{B}$ <sup>28,30</sup>. The corresponding energy dispersion and wavefunction are, respectively,  $E_{\eta,\mathbf{k}} = t_x k_x + t_y k_y + \eta v_F k$ , and  $|u_{\eta}(\mathbf{k})\rangle = 1/\sqrt{2} \begin{bmatrix} 1 & \eta e^{i\Theta_{\mathbf{k}}} \end{bmatrix}^T$ , where  $\eta = \pm$  for the conduction and valence bands, and  $\Theta_{\mathbf{k}} = \eta \arg(-k_y + ik_x)$  is the phase of wavefunction and also the azimuthal angle of the in-plane spin vector. The modification of TISS by an in-plane magnetic field is clear by comparing the electronic structures at  $\mathbf{B} = \mathbf{0}$  [cf. Fig. 2(c)] and  $\mathbf{B} \neq \mathbf{0}$  [cf. Fig. 2(e)]. Using the standard  $T$ -matrix approach<sup>32,48</sup>, the FO or the change of local DOS (LDOS) with energy and space resolution is given as<sup>36,49</sup>

$$\delta\varrho_{\alpha\beta}(\varepsilon, \mathbf{r}) = -\frac{1}{\pi} \text{Im Tr}[\mathbf{g}(\varepsilon, \mathbf{r})\mathbf{T}_{\alpha}\mathbf{g}(\varepsilon, -\mathbf{r})\sigma_{\beta}], \quad (10)$$

where the  $T$ -matrix is expressed as

$$\mathbf{T}_{\alpha}(\varepsilon) = \mathbf{V}_{\alpha} [1 - \mathbf{g}(\varepsilon, \mathbf{0})\mathbf{V}_{\alpha}]^{-1}, \quad (11)$$

with  $\mathbf{V}_{\alpha}$  from the impurity potential. Here, we use the subscript  $\alpha \in \{0, x, y, z\}$  with  $\alpha = 0$  and  $\alpha \neq 0$  for the spin-unpolarized and spin-polarized imperfection or STM tip, respectively, so  $\delta\varrho_{\alpha\beta}(\varepsilon, \mathbf{r})$  gives  $\beta$ -resolved LDOS induced by  $\alpha$ -resolved imperfection. The derivation of real-space GF is the prerequisite to analyse  $\delta\varrho_{\alpha\beta}(\varepsilon, \mathbf{r})$ , which is usually hard for the model Hamiltonian<sup>50</sup> and time-consuming for the electronic structure of first-principle calculations<sup>51</sup>. However, the ultimate expression of GF (i.e., Eq. (8)) can be conveniently derived once the CEC is given, even for the first-principle electronic structure. To utilize Eq. (8) for the Hamiltonian Eq. (9), we first need to derive the stationary points  $\mathbf{k}_c = (k_{x,c}, k_{y,c})$ . To consider the Fermi level in the conduction band, the group velocity is  $\mathbf{v} = (v_x, v_y)$  with  $v_{x,y} = t_{x,y} + v_F k_{x,y}/k$ . On the stationary points,  $\mathbf{v} \parallel \mathbf{r}$ , so  $v_y/v_x = \tan\theta_r$  which gives the equation for  $\mathbf{k}$ . Combining the energy dispersion  $E_{\eta,\mathbf{k}} = \varepsilon$  for given Fermi level  $\varepsilon$ , we obtain

$$k_{x,c}(\theta_r) = \frac{\varepsilon}{v_r^2 v_m} \left[ t_x t_y \sin\theta_r + (v_F^2 - t_y^2) \cos\theta_r - v_m t_x \right] \quad (12a)$$

$$k_{y,c}(\theta_r) = \frac{\varepsilon}{v_r^2 v_m} \left[ t_x t_y \cos\theta_r + (v_F^2 - t_x^2) \sin\theta_r - v_m t_y \right], \quad (12b)$$

where  $v_m = \sqrt{v_F^2 - t^2 \sin^2(\phi - \theta_r)}$  with  $\phi = \arg(t_x + it_y)$ , and  $v_r^2 = (v_F^2 - t_x^2 - t_y^2)$ . Then one can obtain the classic velocity  $\mathbf{v}_c(\mathbf{r})$  and then its magnitude  $v_c = |\mathbf{v}_c| = t \cos(\theta_r - \phi) + v_m$ . In addition, the curvature of CEC corresponding to the energy dispersion is  $\kappa(\theta_r) = v_m^3/\varepsilon v_F^2$ . According to Eq. (8), the explicit expression of GF is

$$\mathbf{g}(\varepsilon, \pm\mathbf{r}) = c_{\pm} e^{ik_{c,\pm}r} \begin{bmatrix} 1 & e^{-i\Theta_{\pm}} \\ e^{i\Theta_{\pm}} & 1 \end{bmatrix}, \quad (13)$$

where  $c_{\pm} = -ie^{-i\pi/4} \sqrt{\pi\rho_{\pm}/(2v_{c,\pm}r)}$  with  $\rho_{\pm} = (4\pi^2 v_{c,\pm} \kappa_{\pm})^{-1}$ . Here, to account for  $\pm\mathbf{r}$ , we define  $k_{c,\pm} = k_{x,c}(\theta_{\pm r}) \cos\theta_{\pm r} +$

$k_{y,c}(\theta_{\pm\mathbf{r}})\sin\theta_{\pm\mathbf{r}}$ ,  $\mathbf{v}_{c,\pm} = \mathbf{v}_c(\pm\mathbf{r})$ ,  $\kappa_{\pm} = \kappa(\theta_{\pm\mathbf{r}})$ , and  $\Theta_{c,\pm} = \Theta_{\mathbf{k}_{c,\pm}}$ . To arrive at the explicit expression of GF, the LDOS can be conveniently derived by incorporating the impurity potential<sup>32</sup>. To intentionally introduce the single impurity<sup>8,9,52</sup>, the precise STM measurements will extract the information on the electronic structure of the host system. In STM study, the conventional processes to characterize the electronic structure are<sup>6</sup>: 1) probing the LDOS with the resolution of the energy and position. 2) performing the Fourier transform of LDOS to obtain experimental quasiparticle interference (QPI). 3) Comparing the experimental QPI to theoretical QPI simulated based on the first-principle or approximate electronic structures. To simulate the QPI,  $T$ -matrix approach and joint DOS (JDOS) approximations are two available methods, and the former is more accurate useful for the approximate electronic structure while the latter is rather rough but used more widely due to its support for the first-principle electronic structure. Our ultimate physical expression of real-space GF favors the straightforward comparison of LDOS between the experiments and simulations by using  $T$ -matrix approach even based on the first-principles electronic structure, this should revolutionize the theoretical understanding of STM measurement.

Back to Eq. (11), the furthermore calculations need the information of impurity potential. In our focus, we intend to present the explicit expressions for the LDOS  $\delta\varrho_{\alpha\beta}(\varepsilon, \mathbf{r})$ . To describe the imperfection as a  $\delta$ -function potential  $\mathbf{V}_\alpha\delta(\mathbf{r})$  with  $\mathbf{V}_\alpha = \mathcal{V}\sigma_\alpha$ ,  $\delta\varrho_{\alpha\beta}(\varepsilon, \mathbf{r})$  will have a explicit form in the Born approximation<sup>48</sup>. For example, adopting  $\mathbf{V}_\alpha = \mathcal{V}\sigma_z$ , we obtain

$$\delta\varrho_{z0} \approx \delta\varrho_{a,z0} \sin(k_+r), \delta\varrho_{a,z0} \equiv C \sin(\Theta_- - \Theta_+), \quad (14a)$$

$$\delta\varrho_{zx} \approx \delta\varrho_{a,zx} \sin(k_+r), \delta\varrho_{a,zx} \equiv C (\sin\Theta_- - \sin\Theta_+), \quad (14b)$$

$$\delta\varrho_{zy} \approx \delta\varrho_{a,zy} \sin(k_+r), \delta\varrho_{a,zy} \equiv C (\cos\Theta_+ - \cos\Theta_-), \quad (14c)$$

$$\delta\varrho_{zz} \approx \delta\varrho_{a,zz} \cos(k_+r), \delta\varrho_{a,zz} \equiv C - C \cos(\Theta_- - \Theta_+), \quad (14d)$$

where  $C = 2\mathcal{V}v_{c,+}c_-/\pi = -(\mathcal{V}/r)\sqrt{\rho_+\rho_-}/(v_{c,+}v_{c,-})$ ,  $k_+ = k_{c,+} + k_{c,-}$  and  $\delta\varrho_{a,\alpha\beta}$  is the amplitude of  $\delta\varrho_{\alpha\beta}$ . If one finishes the measurement of the LDOS induced by the designed imperfection, it is convenient to compare with our theoretical simulations, which help determine the Hamiltonian parameters of  $v_F$  and  $\mathbf{t}$ , and then all physical quantities through the Hamiltonian, e.g., CEC and the group velocities  $v_{c,\pm}$ . This real-space comparison is usually impossible since it is difficult to obtain the real-space GF. In particular, the impurity potential strength  $\mathcal{V}$  may be firstly extracted by performing the same STM probe at zero magnetic field. In contrast to the QPI understanding of STM measurement resorting to the reciprocal space, our theoretical understanding is in real space and more intuitive.

The spin texture embodying in the phase of wavefunction is one of the most remarkable property of TISS, which usually is probed by the ARPES<sup>6,53,54</sup>. To our knowledge, there is no experimental measurement of spin texture by using STM. However, the GDOS, through the amplitude of GF, can realize the STM measurement of the spin texture [cf. black arrows in Fig. 2(d, f)] and even the curvature texture [cf. red arrows in Fig. 2(d, f)]. Thus, our explicit derivations favors the extrac-

tion of the spin texture on the arbitrary position of CEC [cf. Fig. 2(b)], which surpasses previous theoretical simulations of STM measurement<sup>6</sup>.  $\delta\varrho_{a,z\beta}$  implies

$$C = \frac{\delta\varrho_{a,zx}^2 + \delta\varrho_{a,zy}^2}{2\delta\varrho_{a,zz}}, \quad (15a)$$

$$\cos(\Theta_+ - \Theta_-) = 1 - \frac{\delta\varrho_{a,zx}^2 + \delta\varrho_{a,zy}^2}{2C^2}, \quad (15b)$$

$$\cos(\Theta_+ + \Theta_-) = \frac{\delta\varrho_{a,zx}^2 - \delta\varrho_{a,zy}^2}{\delta\varrho_{a,zx}^2 + \delta\varrho_{a,zy}^2}. \quad (15c)$$

Therefore, the azimuthal angle  $\Theta_{\pm}$  of the spin states on the stationary points  $\mathbf{k}_{c,\pm}$  can be solved. To shift the STM tip around the imperfection, one can determine the spin texture on the arbitrary points of the CEC. Nontrivially, the construction of spin texture does not require the input of the information from the Hamiltonian except assuming a spin-1/2 model.

Our theoretical derivations can go further. In particular,  $\kappa_+ = \kappa_- \equiv \kappa_0$  for Eq. (9), so Eq. (15a) can also be used to determine the curvature since

$$C = -\frac{\mathcal{V}}{4\pi^2 r} \frac{1}{\kappa_0 v_{c,+} v_{c,-}}, \quad (16)$$

and  $v_{c,\pm}$  should be given through the CEC construction as discussed previously. To fringe the curvature  $\kappa_0$  on the CEC, the curvature texture is given. In our opinion, it is a promising direction to explore the geometrical curvature texture of the CEC, since it can be constructed through the STM measurement.

*Conclusions.*—In this study, we introduce a geometrical amplitude for locally describing the electronic band structure, namely the GDOS. Comparing to the conventional DOS  $\rho(\varepsilon)$ , the GDOS  $\rho(\varepsilon, \theta)$  obviously provides the information with the higher complexity, as an elegant concept to understand the electronic structure from the local perspective. The GDOS simplifies the construction of real-space GF as the basis for local responses and makes it attain the ultimate expression with clear physics. In particular, in light of the Fermi-surface property, the GDOS could be routinely calculated for the first-principle band structures and furthermore favor the modular calculations of ultimate expression of the real-space GF, this provide a straightforward way to perform the theoretical simulations of STM experiment. In particular, incorporating the ultimate real-space GF into the  $T$ -matrix approach helps build the theoretical formulas for measuring the phase information (i.e., spin texture and curvature texture of CEC) through the amplitudes of STM measurement. Finally, the GDOS should be an universal concept in periodic system, such as photonic crystal, phononic crystal, and so on.

*Acknowledgements.*—This work was supported by the National Key R&D Program of China (Grant No. 2017YFA0303400), the NSFC (Grants No. 12174019, and No. 11774021), and the NSFC program for “Scientific Research Center” (Grant No. U1530401). S.H.Z. is also supported by “Young Talent Program” of BUCT. We acknowledge the computational support from the Beijing Computational Science Research Center (CSRC).

- \* shuhuizhang@mail.buct.edu.cn  
† wenyang@csrc.ac.cn  
‡ kchang@semi.ac.cn
- <sup>1</sup> C. Kittel, *Introduction to Solid State Physics, 8th ed* (Wiley, New York, 2005).
  - <sup>2</sup> M. V. Berry, Proceedings of the Royal Society of London. A. Mathematical and Physical Sciences **392**, 45 (1984).
  - <sup>3</sup> Cohen, Eliahu and Larocque, Hugo and Bouchard, Frederic and Nejdassattari, Farshad and Gefen, Yuval and Karimi, Ebrahim, Nature Reviews Physics **1**, 437 (2019).
  - <sup>4</sup> D. Xiao, M.-C. Chang, and Q. Niu, Rev. Mod. Phys. **82**, 1959 (2010).
  - <sup>5</sup> D. Vanderbilt, *Berry Phases in Electronic Structure Theory: Electric Polarization, Orbital Magnetization and Topological Insulators* (Cambridge University Press, 2018).
  - <sup>6</sup> J.-X. Yin, S. H. Pan, and M. Zahid Hasan, Nature Reviews Physics **3**, 249 (2021).
  - <sup>7</sup> C. Zhang, Z. Yi, and W. Xu, Materials Futures **1**, 032301 (2022).
  - <sup>8</sup> C. Dutreix, H. Gonzalez-Herrero, I. Brihuega, M. I. Katsnelson, C. Chapelier, and V. T. Renard, Nature **574**, 219 (2019).
  - <sup>9</sup> Y. Zhang, Y. Su, and L. He, Phys. Rev. Lett. **125**, 116804 (2020).
  - <sup>10</sup> C. Dutreix, H. González-Herrero, I. Brihuega, M. I. Katsnelson, C. Chapelier, and V. T. Renard, Comptes Rendus. Physique **22**, 133 (2021).
  - <sup>11</sup> A. H. Castro Neto, F. Guinea, N. M. R. Peres, K. S. Novoselov, and A. K. Geim, Rev. Mod. Phys. **81**, 109 (2009).
  - <sup>12</sup> W. Han, R. K. Kawakami, M. Gmitra, and J. Fabian, Nature Nanotechnology **9**, 794 (2014).
  - <sup>13</sup> R. Wang, X.-G. Ren, Z. Yan, L.-J. Jiang, W. E. I. Sha, and G.-C. Shan, Frontiers of Physics **14**, 13603 (2018).
  - <sup>14</sup> Y. Liu, N. O. Weiss, X. Duan, H.-C. Cheng, Y. Huang, and X. Duan, Nature Reviews Materials **1**, 16042 (2016).
  - <sup>15</sup> D. Akinwande, C. Huyghebaert, C.-H. Wang, M. I. Serna, S. Goossens, L.-J. Li, H.-S. P. Wong, and F. H. L. Koppens, Nature **573**, 507 (2019).
  - <sup>16</sup> K. S. Novoselov, A. Mishchenko, A. Carvalho, and A. H. Castro Neto, Science **353**, aac9439 (2016).
  - <sup>17</sup> A. Avsar, H. Ochoa, F. Guinea, B. Özyilmaz, B. J. van Wees, and I. J. Vera-Marun, Rev. Mod. Phys. **92**, 021003 (2020).
  - <sup>18</sup> M. Y. Toriyama, A. M. Ganose, M. Dylla, S. Anand, J. Park, M. K. Brod, J. M. Munro, K. A. Persson, A. Jain, and G. J. Snyder, Materials Today Electronics **1**, 100002 (2022).
  - <sup>19</sup> L. Simon, C. Bena, F. Vonau, M. Cranney, and D. Aubel, J. Phys. D: Appl. Phys. **44**, 464010 (2011).
  - <sup>20</sup> C. Bena, Comptes Rendus Physique **17**, 302 (2016).
  - <sup>21</sup> L. Chen, P. Cheng, and K. Wu, J. Phys. Condens. Matter **29**, 103001 (2017).
  - <sup>22</sup> N. Avraham, J. Reiner, A. Kumar-Nayak, N. Morali, R. Batabyal, B. Yan, and H. Beidenkopf, Advanced Materials **30**, 1707628 (2018).
  - <sup>23</sup> H. Zheng and M. Z. Hasan, Advances in Physics: X **3**, 1466661 (2018).
  - <sup>24</sup> C.-L. Lin, N. Kawakami, R. Arafune, E. Minamitani, and N. Takagi, Journal of Physics: Condensed Matter **32**, 243001 (2020).
  - <sup>25</sup> K. Sato, L. Bergqvist, J. Kudrnovský, P. H. Dederichs, O. Eriksson, I. Turek, B. Sanyal, G. Bouzerar, H. Katayama-Yoshida, V. A. Dinh, et al., Rev. Mod. Phys. **82**, 1633 (2010).
  - <sup>26</sup> S. R. Power and M. S. Ferreira, Crystals **3**, 49 (2013).
  - <sup>27</sup> M. Settnes, S. R. Power, D. H. Petersen, and A.-P. Jauho, Phys. Rev. Lett. **112**, 096801 (2014).
  - <sup>28</sup> S.-H. Zheng, H.-J. Duan, J.-K. Wang, J.-Y. Li, M.-X. Deng, and R.-Q. Wang, Phys. Rev. B **101**, 041408 (2020).
  - <sup>29</sup> W. Rao, Y.-L. Zhou, Y.-j. Wu, H.-J. Duan, M.-X. Deng, and R.-Q. Wang, Phys. Rev. B **103**, 155415 (2021).
  - <sup>30</sup> S.-B. Zhang, C.-A. Li, F. Peña Benitez, P. Surówka, R. Moessner, L. W. Molenkamp, and B. Trauzettel, Phys. Rev. Lett. **127**, 076601 (2021).
  - <sup>31</sup> M. P. do Carmo, *Differential Geometry of Curves and Surfaces* (Dover Publications, New York, 2016).
  - <sup>32</sup> Supplementary Materials (????).
  - <sup>33</sup> E. N. Economou, *Green's Functions in Quantum Physics* (Springer, Berlin, 1983).
  - <sup>34</sup> L. M. Roth, H. J. Zeiger, and T. A. Kaplan, Phys. Rev. **149**, 519 (1966).
  - <sup>35</sup> S. Lounis, P. Zahn, A. Weismann, M. Wenderoth, R. G. Ulbrich, I. Mertig, P. H. Dederichs, and S. Blügel, Phys. Rev. B **83**, 035427 (2011).
  - <sup>36</sup> Q. Liu, X.-L. Qi, and S.-C. Zhang, Phys. Rev. B **85**, 125314 (2012).
  - <sup>37</sup> X.-L. Qi and S.-C. Zhang, Rev. Mod. Phys. **83**, 1057 (2011).
  - <sup>38</sup> P. Roushan, J. Seo, C. V. Parker, Y. S. Hor, D. Hsieh, D. Qian, A. Richardella, M. Z. Hasan, R. J. Cava, and A. Yazdani, Nature **460**, 1106 (2009).
  - <sup>39</sup> J. Seo, P. Roushan, H. Beidenkopf, Y. S. Hor, R. J. Cava, and A. Yazdani, Nature **466**, 343 (2010).
  - <sup>40</sup> P. Sessi, F. Reis, T. Bathon, K. A. Kokh, O. E. Tereshchenko, and M. Bode, Nature Communications **5**, 5349 (2014).
  - <sup>41</sup> S. Jeon, B. B. Zhou, A. Gyenis, B. E. Feldman, I. Kimchi, A. C. Potter, Q. D. Gibson, R. J. Cava, A. Vishwanath, and A. Yazdani, Nature Materials **13**, 851 (2014).
  - <sup>42</sup> H. Beidenkopf, P. Roushan, J. Seo, L. Gorman, I. Drozdov, Y. S. Hor, R. J. Cava, and A. Yazdani, Nature Physics **7**, 939 (2011).
  - <sup>43</sup> I. Zeljkovic, Y. Okada, C.-Y. Huang, R. Sankar, D. Walkup, W. Zhou, M. Serbyn, F. Chou, W.-F. Tsai, H. Lin, et al., Nature Physics **10**, 572 (2014).
  - <sup>44</sup> I. Lee, C. K. Kim, J. Lee, S. J. L. Billinge, R. Zhong, J. A. Schneeloch, T. Liu, T. Valla, J. M. Tranquada, G. Gu, et al., Proceedings of the National Academy of Sciences **112**, 1316 (2015).
  - <sup>45</sup> T. Zhang, P. Cheng, X. Chen, J.-F. Jia, X. Ma, K. He, L. Wang, H. Zhang, X. Dai, Z. Fang, et al., Phys. Rev. Lett. **103**, 266803 (2009).
  - <sup>46</sup> Y. Okada, C. Dhital, W. Zhou, E. D. Hue Miller, H. Lin, S. Basak, A. Bansil, Y.-B. Huang, H. Ding, Z. Wang, et al., Phys. Rev. Lett. **106**, 206805 (2011).
  - <sup>47</sup> S. Kim, S. Yoshizawa, Y. Ishida, K. Eto, K. Segawa, Y. Ando, S. Shin, and F. Komori, Phys. Rev. Lett. **112**, 136802 (2014).
  - <sup>48</sup> E. N. Economou, *Green's functions in quantum physics*, vol. 7 (Springer Science & Business Media, 2006).
  - <sup>49</sup> R. R. Biswas and A. V. Balatsky, Phys. Rev. B **81**, 233405 (2010).
  - <sup>50</sup> M. Istas, C. Groth, and X. Waintal, Phys. Rev. Res. **1**, 033188 (2019).
  - <sup>51</sup> S. Smidstrup, T. Markussen, P. Vancraeyveld, J. Wellendorff, J. Schneider, T. Gunst, B. Verstichel, D. Stradi, P. A. Khomyakov, U. G. Vej-Hansen, et al., Journal of Physics: Condensed Matter **32**, 015901 (2019).
  - <sup>52</sup> H. González-Herrero, J. M. Gómez-Rodríguez, P. Mallet, M. Moaied, J. J. Palacios, C. Salgado, M. M. Ugeda, J.-Y. Veillen, F. Yndurain, and I. Brihuega, Science **352**, 437 (2016).
  - <sup>53</sup> D. Hsieh, Y. Xia, D. Qian, L. Wray, J. H. Dil, F. Meier, J. Osterwalder, L. Patthey, J. G. Checkelsky, N. P. Ong, et al., Nature **460**, 1101 (2009).
  - <sup>54</sup> D. Hsieh, Y. Xia, L. Wray, D. Qian, A. Pal, J. H. Dil, J. Oster-

walder, F. Meier, G. Bihlmayer, C. L. Kane, et al., *Science* **323**, 919 (2009).